



ESA CONTRACT REPORT

Contract Report to the European Space Agency

*Operational Assimilation of Space-borne Radar and
Lidar Cloud Profile Observations for Numerical Weather
Prediction*

**WP-6000 report: Conclusions and
recommendations**

M. Janisková and M. Fielding

ESA ESTEC contract 4000116891/16/NL/LvH

**European Centre for Medium-Range Weather Forecasts
Europäisches Zentrum für mittelfristige Wettervorhersage
Centre européen pour les prévisions météorologiques à moyen terme**



ECMWF

Series: ECMWF ESA Project Report Series

A full list of ECMWF Publications can be found on our web site under:

<http://www.ecmwf.int/en/research/publications>

Contact: library@ecmwf.int

©Copyright 2018

European Centre for Medium Range Weather Forecasts
Shinfield Park, Reading, RG2 9AX, England

Literary and scientific copyrights belong to ECMWF and are reserved in all countries. This publication is not to be reprinted or translated in whole or in part without the written permission of the Director-General. Appropriate non-commercial use will normally be granted under the condition that reference is made to ECMWF.

The information within this publication is given in good faith and considered to be true, but ECMWF accepts no liability for error, omission and for loss or damage arising from its use.

Contract Report to the European Space Agency

*Operational Assimilation of Space-borne Radar and Lidar Cloud
Profile Observations for Numerical Weather Prediction*

WP-6000 report: Conclusions and recommendations

Authors: M. Janisková and M. Fielding

ESA ESTEC contract 4000116891/16/NL/LvH

June 2018

ABSTRACT

This report provides a summary of developments and experimentation studies towards monitoring and assimilation of space-borne radar and lidar cloud profile observations in Numerical Weather Prediction (NWP) model.

An overview of the required adjustments of assimilation tools, such as the observation operators, observation error definition, quality control, data screening and bias correction, in order to build a direct data assimilation and monitoring system for such observations is provided.

Conclusions from monitoring experiments for cloud radar and lidar observations using CloudSat (NASA's cloud radar mission) and CALIPSO (Cloud-Aerosol Lidar and Infrared Pathfinder Satellite Observations) data have suggested that the skill of monitoring system to detect a degradation in the quality of observations is improved when the first guess departures are used compared to using just observations alone.

Outcomes from 4D-Var assimilation experiments using CloudSat cloud radar reflectivity and CALIPSO lidar backscatter observations, either separately or in combination indicated that Four-Dimensional Variational (4D-Var) analyses get closer to assimilated observations. However, impact of the cloud radar reflectivity is larger than that of the lidar backscatter. Impact on the first-guess (FG) and analysis (AN) departure statistics when verified against other observation types assimilated in 4D-Var is most pronounced and positive for conventional observations, especially for wind. An impact of the new observations on the subsequent forecast is largest for zonal wind, relative to both operational analysis and conventional observations, such as radiosonde or aircraft data. Results also indicated an improved forecast, especially rain rates in the tropics.

Suggested perspectives for the future assimilation and a brief summary of work still required to complete a preparation for possible operational assimilation and monitoring of the EarthCARE radar and lidar cloud observations are also provided.

Contents

1	Introduction	1
2	Conclusions and recommendations from developments for observation processing	2
2.1	Observation operator developments and updates	2
2.2	Observation pre-processing	3
2.2.1	Bias correction	3
2.2.2	Observation error	4
2.3	Adjustments required for the EarthCARE observations	6
3	Conclusions and recommendations for data monitoring of cloud radar and lidar observations	7
3.1	Performed experiments	7
3.2	Summary and perspectives	8
4	Conclusions and recommendations from data assimilation experiments for radar and lidar	10
4.1	Performed experiments	10
4.2	Summary of the results	10
4.2.1	Impact on the analysis	10
4.2.2	Impact on the subsequent forecast	13
4.3	Perspectives	15
5	Required work towards monitoring and assimilation of EarthCARE radar and lidar observations	18
6	Brief analysis of possible benefits of using EarthCARE MSI observations for assimilation	19

1 Introduction

Over the past few years the representation of precipitation and clouds in global Numerical Weather Prediction (NWP) models has greatly improved and has reached a reasonable degree of realism. This opens new possibilities for improvements of the atmospheric initial state and the model performance itself to be explored through assimilation of data related to clouds from active and passive instruments. Observations providing vertical information on clouds from space-borne active instruments on board of CloudSat ([Stephens et al., 2002](#)) and CALIPSO (Cloud-Aerosol Lidar and Infrared Pathfinder Satellite Observations [Winker et al., 2009](#)) are already available and new ones, such as Earth, Clouds, Aerosols and Radiation Explorer (EarthCARE, [Illingworth et al., 2015](#)) should appear in the near future. The EarthCARE mission will provide the vertically resolved characterization of clouds by the combination of lidar (Atmospheric Lidar, ATLID) and a cloud profiling radar (CPR) as described in the ESA report ([ESA, 2004](#)).

A number of studies, including the ESA funded project Quantitative Assessment of the Operational Value of Space-Borne Radar and Lidar Measurements of Cloud and Aerosol Profiles (QuARL [Janisková et al., 2010](#)), have shown that observations of clouds from space-borne radar and lidar are useful not only to evaluate the performance of current NWP models in representing clouds, precipitation and aerosols, but they have also the potential to be assimilated into these models to improve their initial atmospheric state. The subsequent study (STSE Study - EarthCARE Assimilation, [Janisková et al., 2014](#)) focused on the development of an off-line system to monitor/assimilate space-borne radar and lidar observations in clouds within the NWP model of the European Centre for Medium-Range Weather Forecasts (ECMWF) in order to prepare for the exploitation of radar and lidar observations in data assimilation. The studies using a technique combining one-dimensional variational (1D-Var) assimilation with four-dimensional variational (4D-Var) data assimilation provided indications on the potential that assimilation of cloud information from active sensors could offer. However, they also suggested that the 1D+4D-Var approach is quite expensive for profiling observations and not affordable for operational applications due to the costly definition of errors for the pseudo-observations retrieved from 1D-Var by computing them from the 1D-Var analysis covariance matrix. Therefore for any future operational implementation, the use of a direct 4D-Var assimilation of cloud related observations needs to be rather considered. A necessary additional activity to assimilation is to add a quality monitoring system using a global NWP model, which is an important step before any observations can be assimilated into 4D-Var.

Following the previous studies, the current project has focused on developments towards direct assimilation and monitoring systems to exploit cloud radar and lidar data for their assimilation in NWP models. The direct (in-line) data assimilation and monitoring systems developed during this project allow extended research studies beneficial for future applications of EarthCARE ATLID and CPR data once available on the global scale.

Building direct data assimilation and monitoring systems for space-borne cloud radar and lidar observations required adjustment of assimilation tools developed during the STSE Study - EarthCARE Assimilation ([Janisková et al., 2014](#)), such as observation operator, observation error definitions (namely, representativeness and forward operator errors), quality control, data screening and bias correction. The updates to the observation operator, specifically the microphysical assumptions to provide physical consistency with the Integrated Forecasting System (IFS) cloud scheme and alternative approach to account for cloud overlap, are described in WP-2000 (Observation quality monitoring and pre-processing, [Fielding and Janisková, 2017a](#)). In the same work package, a new flow-dependent representativity error method has been introduced. A bias correction scheme using the updated model configuration and customized indicators has been also implemented. Finally, the automatic monitoring system has been introduced and demonstrated off-line in WP-2000 as well.

The technical developments related to the handling of the actual observations have been given in WP-3000 (Assimilation system development for cloud radar and lidar observations, [Janisková et al., 2017](#)). This report also described the developments to the assimilation system at ECMWF in preparation for the inclusion

of cloud radar and lidar data directly into the 4D-Var system. The specific modifications to the assimilation system required for the EarthCARE cloud radar and lidar data are summarized in WP-4000 (EarthCARE data handling and testing, [Fielding et al., 2017](#)). Based on the differences between EarthCARE observations compared to CloudSat and CALIPSO data, updates to the forward model the off-line observation handling of raw EarthCARE L1b data into Binary Universal Format (BUFR) have been made.

Finally, the feasibility of assimilating CloudSat cloud radar reflectivity and CALIPSO lidar backscatter observations into a global NWP model has been demonstrated in WP-5000 (Feasibility demonstration of 4D-Var assimilation system using CloudSat and CALIPSO observations, [Janisková and Fielding, 2018](#)).

In this report, Section 2 provides conclusions and recommendations from developments for observation processing, such as observation operator developments and updates, observation preprocessing, as well as summary of adjustments for the EarthCARE observations. Conclusions and recommendations for data monitoring of cloud radar and lidar observations are outlined in Section 3. Outcomes from data assimilation experiments for these observations are presented in Section 4 together with the suggested perspectives for the future assimilation of those data. Section 5 briefly summarizes the work required to complete a preparation for possible operational monitoring and/or assimilation of the EarthCARE radar and lidar cloud observations. Finally, a short analysis of possible benefits using EarthCARE Multi-Spectral Imager (MSI) observations for assimilation is provided in Section 6.

2 Conclusions and recommendations from developments for observation processing

2.1 Observation operator developments and updates

The observation operator is a fundamental part of data assimilation as it transforms model variables to observations, thus allowing the model fit to observations to be assessed and improved. The observation operators for radar reflectivity and lidar backscatter within the IFS model were developed in two previous projects (QuARL, [Janisková et al., 2010](#); and STSE Study - EarthCARE Assimilation, [Janisková et al., 2014](#)), however in this current project they have been updated for in-line assimilation, where operational constraints require a balance of efficiency and complexity. There has also been a focus on consistency; the assumptions made in the observation operators have been modified to be consistent with each other, and (as much as possible) consistent with other forward models and parameterizations in the ECMWF 4D-Var assimilation and forecasting systems (IFS). Without consistency, there is the possibility that observation operators for different observation types could work against each other, preventing the model initial state from getting closer to the truth.

Two major updates were made to the operator to improve efficiency. The first was to introduce a parameterization of the hydrometeor scattering properties. In the original version of the operator, the scattering properties were found using a pre-computed look-up table as a function of temperature and in-cloud water content. Through experimentation with different characteristic functions it was found that both radar reflectivity and lidar backscatter could be approximated by a two-variable two-degree polynomial with six fitting coefficients. Using the parameterization was found to be an order of magnitude faster than searching the look-up table. Secondly a much more efficient way to handle cloud overlap was devised. By partitioning the transmission into a cloudy and a clear column, similar results can now be obtained as from the original multi-column method, which requires the computation of at least 20 sub-columns and is not differentiable and therefore was used for monitoring and evaluation only. The development of the double-column method allows cloud overlap to be specified in the data assimilation, which should improve the assimilation of lidar in scenes with strong attenuation, such as multi-layer clouds.

Considering all the updates to the observation operator for radar reflectivity, Fig. 2.1 shows the frequency distribution of radar reflectivity with temperature for CloudSat observations, the previous version of the observation operator and the latest version of the operator. In particular, this figure highlights the new particle size distribution chosen for stratiform rain Abel and Boutle (2012). The new scheme's shift towards smaller drops for smaller water contents results in a significant reduction in radar reflectivity for water content less than 0.01 g m^{-3} , providing a much better fit to observations. Other modifications to the microphysical assumptions of the operator were designed to match those in the IFS cloud scheme and with each other, such as changing the ice cloud particle type for lidar from 'aggregate of columns' to '6-bullet rosette'.

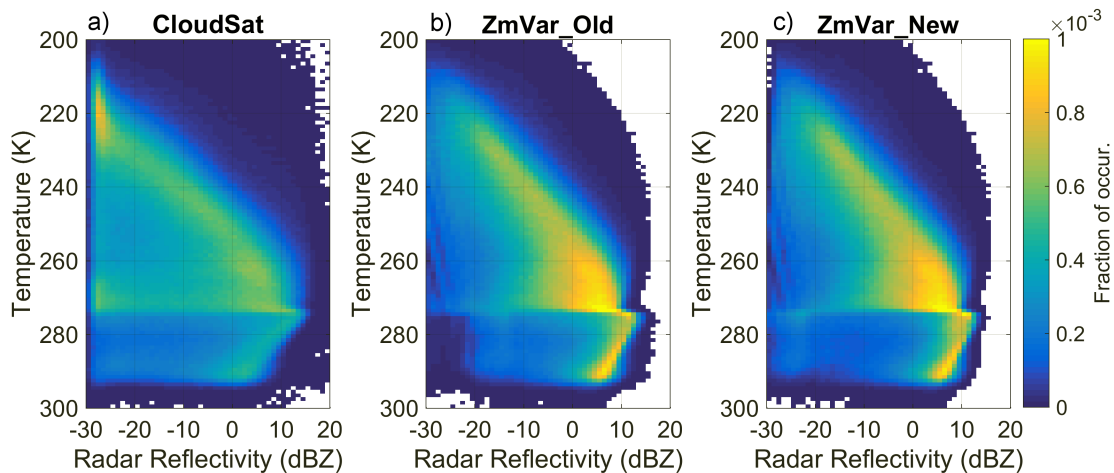


Figure 2.1: Frequency distribution of observed and simulated radar reflectivity with temperature. Panel (a) shows CloudSat observations for August 2007 after averaging at model resolution. Panels (b) and (c) show the simulated reflectivity using the original and updated lookup tables, respectively.

2.2 Observation pre-processing

To enable the in-line assimilation of radar reflectivity and lidar backscatter within the ECMWF 4D-Var assimilation system significant developments, both scientific and technical, were required. Firstly the quality control and bias correction schemes needed to be refined compared to those used in the 1D+4D-Var experiments. Whereas the pseudo-observations of humidity and temperature could be screened in the 1D-Var computation before entering the 4D-Var system, direct radar and lidar profiles cannot, so a more careful screening was required.

Quality control and screening help to prevent observations that will have a negative impact on the data assimilation analysis and subsequent forecast from entering the system. There are several reasons that an observation may not have a positive impact; they may be unphysical, the forward model may not be capable of representing the observation, or they may cause excessive non-linearities in the observation operator. The updated screening indicators are shown in Table 2.1. New screening indicators included the blacklisting of excessively attenuated signals in the lidar backscatter and model levels with small cloud fraction.

2.2.1 Bias correction

Due to the updates in the observation operators and the new screening criteria, a new bias correction scheme was required. A bias correction scheme is an important component of any data assimilation system as it ensures systematic biases, which can have a detrimental impact on the analysis, are removed. The bias correction scheme is based on indicators of height and temperature, thus providing an implicit regime dependence. Joint

Indicator	Min	Max	Reason
Height (km)	1	20	Lower limit (relative to surface) to avoid surface return, upper limit (absolute) to discard spurious signals (although some stratospheric clouds may be removed)
CF_{IFS}	0.2	1.0	To avoid non-linearity and representativity issues
CF_{obs}	0.2	1.0	To avoid non-linearity and representativity
dBZ_{IFS}, dBZ_{obs}	-30	20.0	Plausible bounds for radar
$dB\beta_{IFS}, dB\beta_{obs}$	-50	0.0	Plausible bounds for lidar
FG departures	-20	20	Remove large departures
dBZ_{int}	0.0	41.3	Radar multipile scattering not modelled by observation operator
β_{int}	0.0	0.02	Avoid observations with excessive attenuation

Table 2.1: Screening thresholds for CloudSAT and Calipso observations.

probability density plots of simulated and observed radar reflectivity before and after the bias correction has been applied are shown in Fig. 2.2.

For the radar reflectivity, in a global sense, the difference between observations and model equivalent is remarkably unbiased and a strong correlation (a correlation coefficient of approximately 0.7) is apparent. Two modes can be seen, one in the range -30 to -20 dBZ and one in the range 0 to 5 dBZ, corresponding to areas of ice cloud and precipitation respectively. After bias correction, the slight underestimation of precipitation was corrected and the overestimation of ice cloud reflectivity was reduced. For the lidar backscatter, the difference between observations and model equivalent are greater and the correlation is less than seen for the radar reflectivity. An underestimation in the ice cloud (with first guess around -30 dB β) was corrected by applying bias correction.

The bias correction will need to be recomputed each time either the IFS model or the observation operator is updated as both will affect any systematic biases present. However, as the framework has been constructed, it should be straight-forward to generate, providing the changes do not warrant the selection of different indicators. In an operational context, it would be desirable to use variational bias correction where biases are automatically corrected within 4D-Var, but this would require at least six months of stable observations and significant efforts to ensure the system was performing correctly.

2.2.2 Observation error

To combine the observations and the model, the data assimilation system requires an estimate of the observation error. Following the approach taken in previous projects, we assume that the observation error is a function of measurement error, representativity error and forward model error. By computing these constituent parts, a physically based estimate of the observation error is obtained. To model the representativity error, a new technique is implemented that uses the local variability along the transect combined with correlation from a climatology. The new method has been validated using synthetic data and MODIS radiances (Fielding and Janisková, 2017b) and has similar performance to a more complex method based on look-up tables (Stiller, 2010). To obtain estimates of forward model error, we use a Monte Carlo approach (similar to, e.g., Kulie et al., 2010; Di Michele et al., 2012), where microphysical assumptions are perturbed within their physical ranges. With all components combined, this physically based estimate of observation error has the advantage of being independent from the model background errors and should give a better estimate of the true observation error.

Figure 2.3 shows the mean observation error calculated for one month of CloudSat and CALIPSO observations. For CloudSat radar reflectivity, representativity error tends to dominate over tropical areas, while forward model error dominates the extra-tropics, particularly in stratiform regimes. Conversely, for CALIPSO lidar backscatter, the observation error tends to be less in the tropics as the lidar has the smallest errors for regions associated with ice cloud, such as those formed by convective outflow. The spatial magnitude of observation error for both

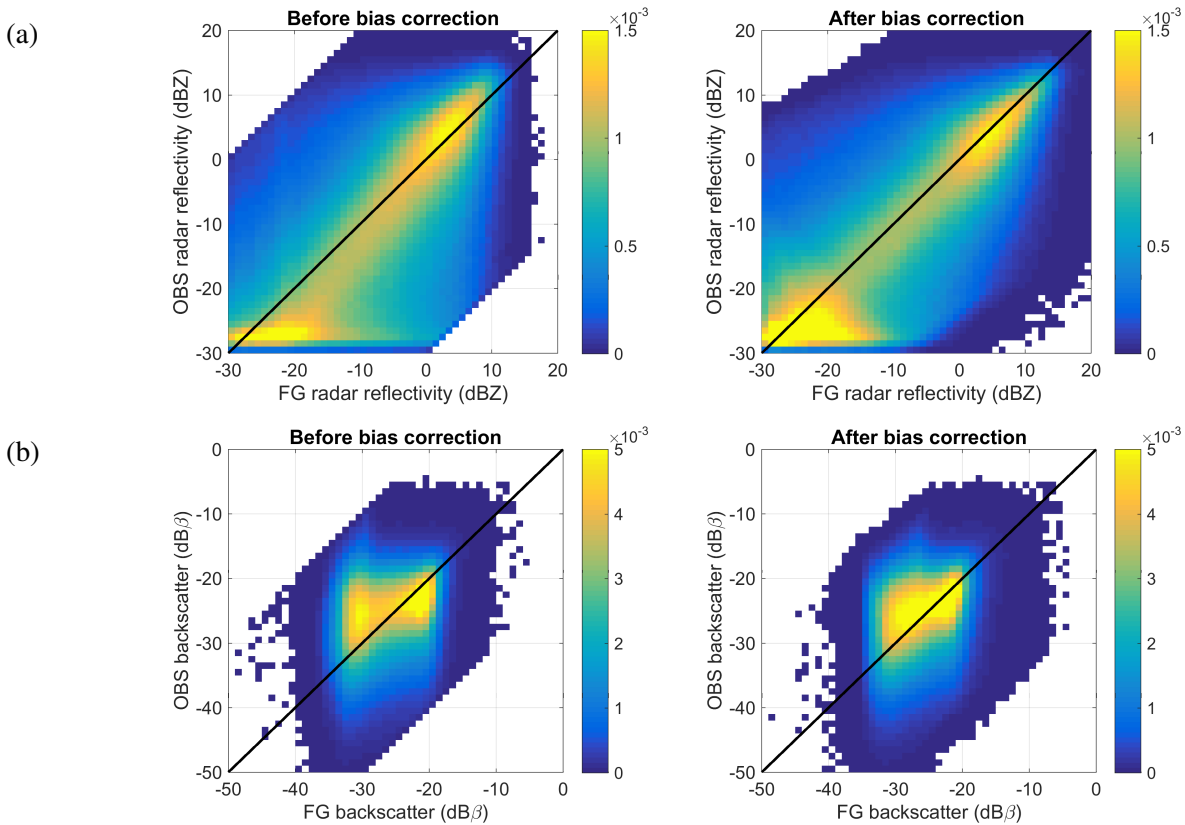


Figure 2.2: Joint probability density plots of (a) simulated radar reflectivity and observed CloudSat radar reflectivity, and (b) simulated lidar backscatter and CALIPSO lidar attenuated backscatter using observations during September 2007. The left panel shows data before bias correction, while the right panel shows the relationship after bias correction. Only data passing quality control are considered.

CloudSat and CALIPSO also compares favourably with the standard deviation of first guess departures.

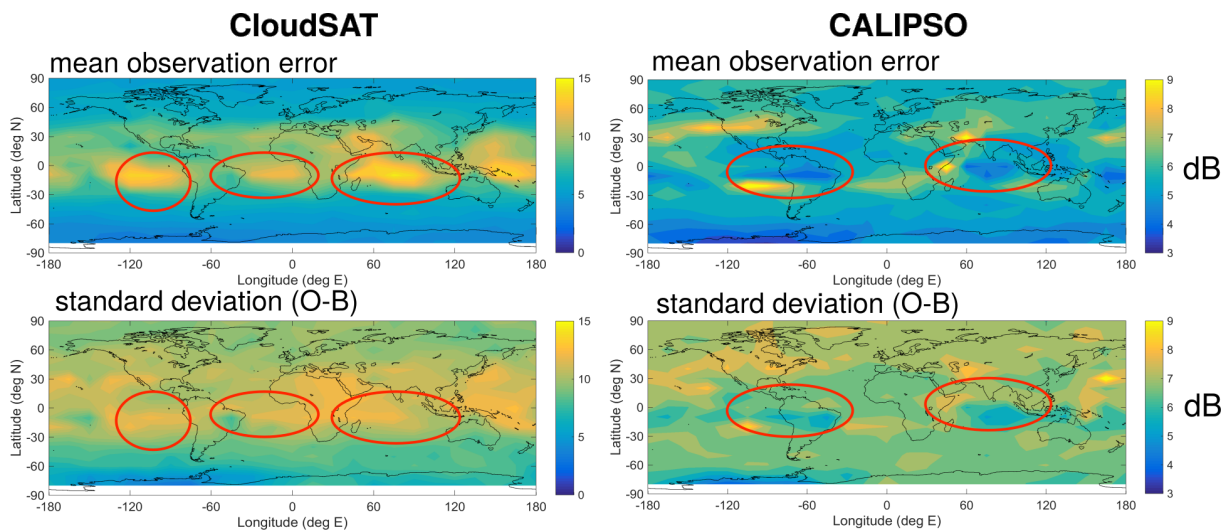


Figure 2.3: A comparison of global maps of CloudSat radar (left side) and CALIPSO lidar (right side) mean expected observation errors (sum of instrument, operator and representativity errors; top) versus the standard deviation of first guess departure errors (bottom). The red ovals are to aid comparison.

2.3 Adjustments required for the EarthCARE observations

The CloudSat radar and CALIOP (Cloud-Aerosol Lidar with Orthogonal Polarization) lidar share many characteristics of the EarthCARE CPR (Cloud Profiling Radar) and ATLID (ATmospheric LIDar) and have been considered synonymous for technical testing and feasibility studies. However, to assimilate the CPR and the ATLID with scientific meaning, several modifications are required and have been prepared for. For the radars, the main differences between the instruments relate to the larger antenna of the CPR, which leads to greater sensitivity and reduced multiple scattering. The CPR also detects the phase shift of signals, such that the Doppler velocity of targets can be measured. For the lidars, the differences are potentially more significant; the wavelength of the instruments are also different, which leads to different cloud and molecular scattering properties. The smaller field of view of the ATLID also leads to reduced multiple scattering.

Specifically, the main conclusions from adapting the forward models to EarthCARE specifications were that:

- The CPR will detect significantly smaller hydrometeors (the 7 dB increase in sensitivity will detect particles with up to 30% smaller radii), which should halve the number of clouds missed (particularly ice clouds) and allow greater synergy with the lidar.
- The sensitivity in total attenuated backscatter is less for ATLID due to the increased molecular backscatter at 355nm compared to CALIPSO.
- The effects of multiple scattering are likely be similar in the two lidars due to compensating effects of ATLID's narrower field of view, yet shorter wavelength.

Technical changes needed to process the EarthCARE data into a format that can be ingested and used by the data assimilation system were also developed. Developments focused on the tools to convert the L1b data format into BUFR, which required the definition of new BUFR descriptors. Some changes to the data selection, pre-processing and screening were needed, particularly in relation to the cloud masks, which will not be provided in the L1b raw data. Tests demonstrating the technical capability of the system to assimilate EarthCARE data were made, making use of the A-NOM and C-NOM test data produced using a high-resolution model and the EarthCARE Simulator ([Fielding et al., 2017](#)).

Some developments will be necessary in the commissioning phase of the EarthCARE mission, particularly in relation to tuning of the bias correction and screening schemes, observation error specification but the framework for assimilating EarthCARE observations is now in place.

3 Conclusions and recommendations for data monitoring of cloud radar and lidar observations

Before any new observations are actively assimilated in the ECMWF 4D-Var system, they are passively monitored, along with all the actively assimilated observations, ensuring that both the observations and model are behaving as expected. Due to the vast quantities of data involved, the monitoring system at ECMWF is automated, where selected indicators are checked against expected ranges. Alerts are automatically triggered and sent to analysts for further investigation if the observations exceed these ranges. In addition, alerts can be sent to other relevant parties, including instrument mentors, which could be critical in detecting and correcting problems with satellite data in a timely manner.

3.1 Performed experiments

Before showing examples of cloud radar and lidar data within the automated monitoring system, indicators were chosen and statistics generated to set the expected ranges of the data. Figure 3.1 shows statistics for 12-hour mean indicators of observation value only and the first guess departures for both radar reflectivity and lidar backscatter. The hard limits, designed to detect drifts in the observations or model are set (red dashed lines) using a threshold in the standard deviation. As the indicators' distributions resemble normal distributions, the data is suitable for monitoring and detecting errors.

To show the power of combining observations and model information within a monitoring system to detect instrument problems, an experiment was carried out where artificial drifts were applied to CloudSat and CALIPSO data. Figure 3.2 shows an example where a 1% decrease per day was applied to the CloudSat radar reflectivity, leading to a total bias of 3 dB after two months. No automatic alerts due to the drift were triggered when considering observations only (Fig. 3.2a), whereas alerts were triggered around 30 days after the bias was introduced when considering the combination of observations and model (Fig. 3.2b).

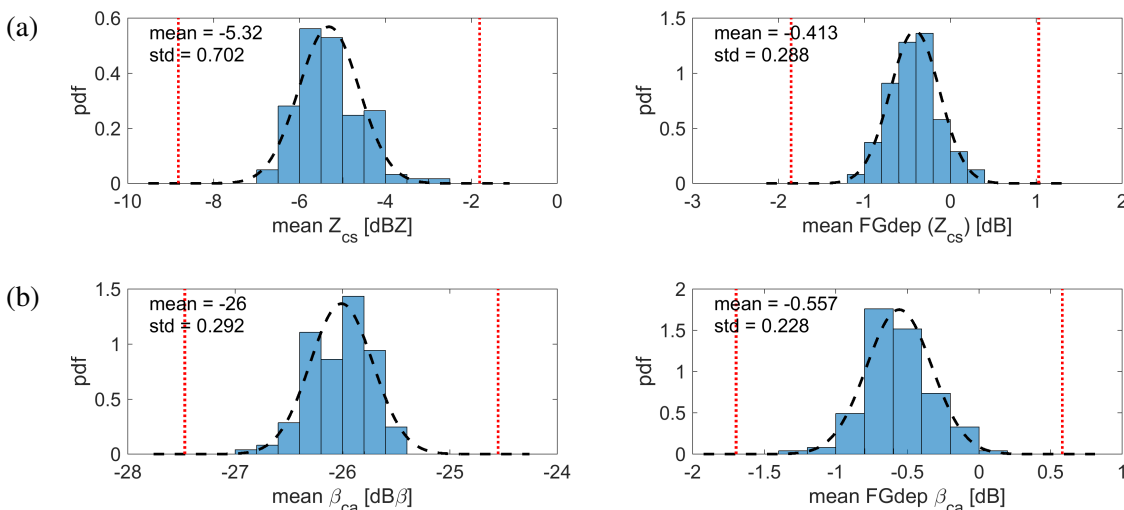


Figure 3.1: Histograms of 12-hour global mean observations and model equivalent related variables for a three month period between August - September 2007. Panels on left side show observation related variables: (a) mean CloudSat radar reflectivity and (b) mean CALIPSO lidar attenuated backscatter. Panels on right side show observation and model related variable - mean first guess departures for (a) radar reflectivity and (b) lidar backscatter. The black dashed line in each panel shows the Gaussian distribution with the mean and standard deviation of the data. The red dotted lines indicate 5 standard deviations from the mean.

A similar conclusion is reached when considering the artificial drift in CALIPSO observations of lidar backscatter (Fig. 3.3). However, in this case, due to the narrow dynamic range of CALIPSO attenuated backscatter compared to CloudSat radar reflectivity, the artificial drift is first detected after 20 days in observations alone. In contrast, using the combination of observations and model the first alarm is triggered after 15 days and the bias is much more apparent with many more alerts triggered by the end of the two month period considered.

3.2 Summary and perspectives

The automatic monitoring system at ECMWF is a powerful tool for analysing the performance of both the model and observations. By considering both observations and model together, we have shown that drifts in the calibration of an instrument can be detected much faster than considering observations alone. In this sense, monitoring of the EarthCARE instruments at ECMWF could provide extremely valuable information for ESA instrument mentors in the timely detection, quantification and correction of instrument problems to minimize the impact on other data users.

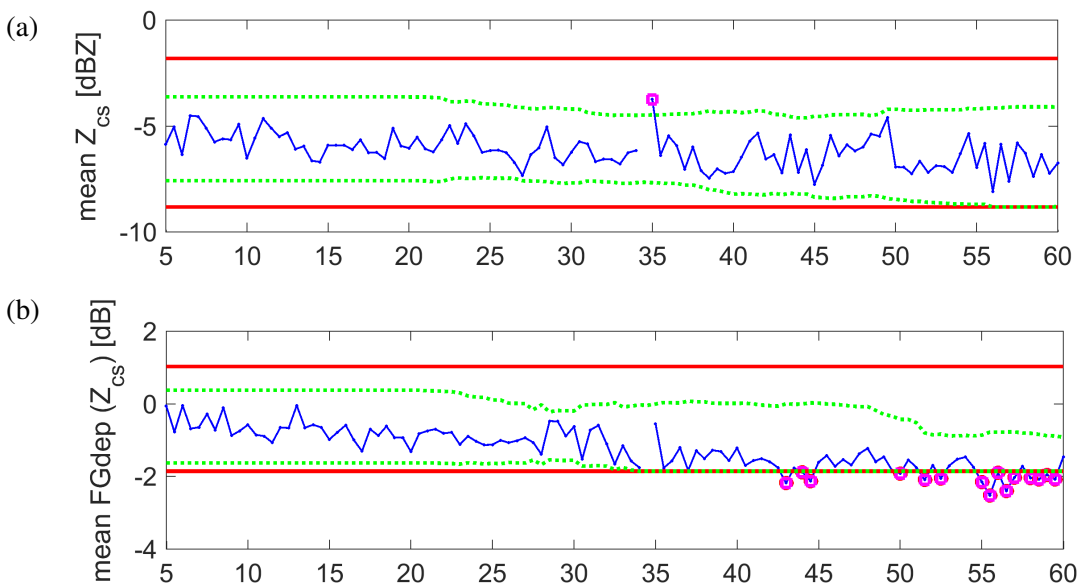


Figure 3.2: Example of CloudSat data within the automatic monitoring system using (a) observation-only indicators of global mean radar reflectivity and (b) using combined observation and model indicators of global mean first guess departures where a 1% per day drift in observed radar reflectivity has been introduced at day 10.

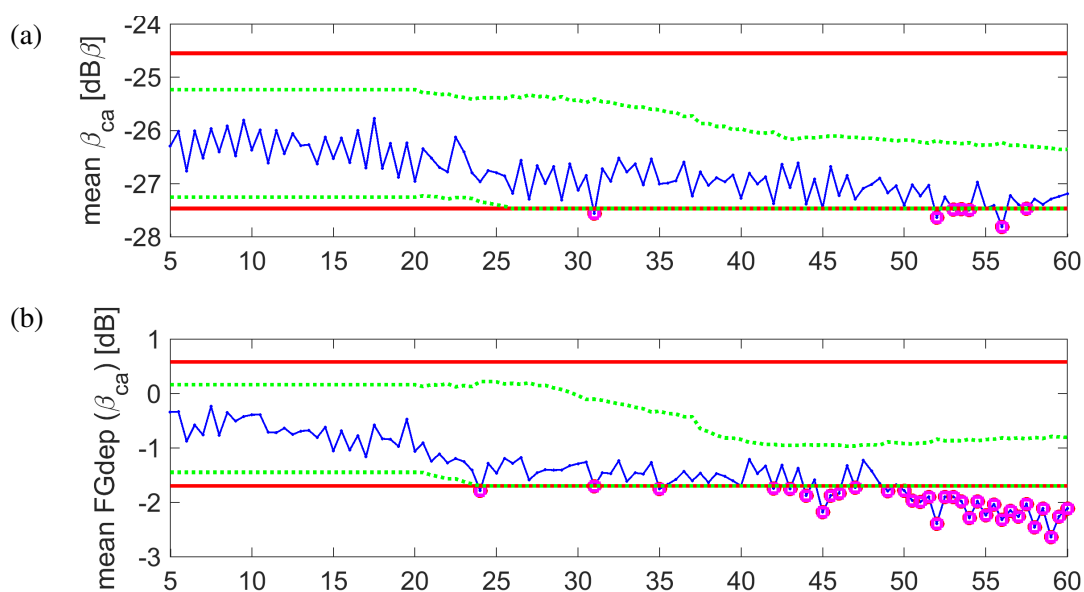


Figure 3.3: Same as Fig. 3.2, but for CALIPSO data of lidar attenuated backscatter.

4 Conclusions and recommendations from data assimilation experiments for radar and lidar

4.1 Performed experiments

In order to study the impact of space-borne cloud radar and lidar observations on analyses and subsequent forecast, 4D-Var assimilation system used at ECMWF has been updated to account for these new observation types. This required a lot of development described in the previous sections, such as modifications and developments to observation operators, observation error definition and data handling for observations (i.e. quality control, screening and bias correction). After technical testing of the correctness of the updated system, 4D-Var assimilation experiments have been performed using cloud radar reflectivity and lidar backscatter. Using the full system of regularly assimilated observations at ECMWF and assimilation cycles of 12-hours (i.e. the current length of 4D-Var assimilation window at ECMWF), several experiments have been performed over 10 days covering 1-10 August 2007 period adding the new observations to the system. 4D-Var experimentation has been done using a horizontal resolution of TCo639 spectral truncation (corresponding to approximately 18 km on a cubic octahedral grid) and 137 vertical levels. Measurements of cloud radar reflectivity (in dBZ), from the CloudSat 94 GHz radar and/or lidar backscatter (in dB, when using logarithmic scale) due to clouds at 532 nm from CALIPSO for the selected situations have been averaged to the model horizontal resolution approximately 36 km. This is twice coarser than experimental horizontal resolution in order to obtain smoother observation field for data assimilation.

Several 4D-Var experiments have been run with different setups to study the impact of the new cloud radar and lidar observations, either each of them separately or together and then without or in combination with other regularly assimilated observations. The impact of observation error definition on the performance has been also investigated.

Impact of added observations on 4D-Var analyses has been investigated by comparing the first-guess departures (differences between observations and the model first guess) against the analysis departures (differences between observations and analysis). Verification of the performed assimilation runs has also been carried out against other assimilated observation types in 4D-Var. Analysis increments of temperature and specific humidity have been evaluated as well since they can provide information about the impact of assimilated observations on the control variables of 4D-Var system.

From obtained 4D-Var analyses, 10 day forecasts have been run to study the impact of these new observations on the subsequent forecasts. The comparisons have been concentrated on the forecast of specific humidity, temperature, wind over the whole globe and precipitation over the tropics.

4.2 Summary of the results

4.2.1 *Impact on the analysis*

The performed experiments have shown that 4D-Var provides analysis departures closer to cloud radar and lidar observations than would be obtained if these observations were not assimilated. Probability distribution function (PDF) of the first-guess (FG) and analysis (AN) departures for the cloud radar reflectivity and lidar backscatter shown on Fig. 4.1 for the different assimilation experiments (as specified in figure caption) indicates that analysis including radar and lidar observations together with all other normally assimilated observations provides better PDF distribution than the reference run. Obviously, the most symmetric PDF shapes are achieved when assimilating just the new observations alone.

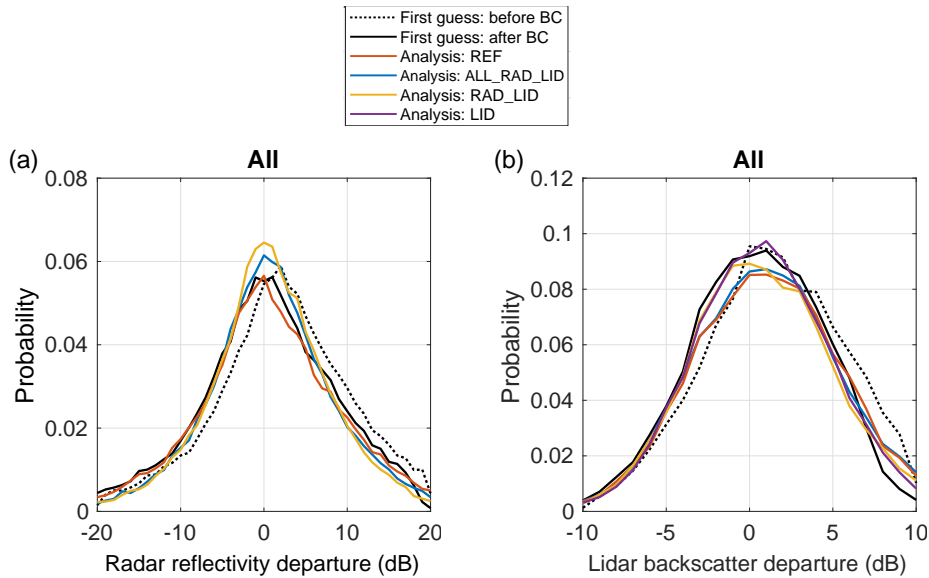


Figure 4.1: Probability distribution functions of the first guess departures before (black dotted line) and after (black solid line) bias correction applied combined with the analysis departures for the reference experiment (**REF**, red solid line), experiment assimilating cloud radar and lidar observations with all other normally assimilated observations (**ALL_RAD_LID**, blue solid line), experiment assimilating cloud radar and lidar observations only (**RAD_LID**, orange solid line) and assimilation using lidar observations only (**LID**, violet solid line). Results are presented for (a) radar reflectivity and (b) lidar backscatter departures (dB) over the whole globe. Situation **2007080100** with 12-hour assimilation period between 31 July 2007 21:00 UTC and 1 August 2007 09:00 UTC.

The fact that analysis is getting closer to the radar and lidar observations has been also demonstrated by along-track evaluation which allowed to investigate the performance of the system in more details by looking at individual clouds. For radar reflectivity, the comparisons clearly showed that despite some discrepancies the first-guess radar reflectivity generated from the background field (Fig. 4.2b) is very similar to the averaged CloudSat radar reflectivity, thus indicating that the model equivalents are sufficient to extract information from the observations. Whereas the fit of the first-guess radar to the observations was impressive, there were greater differences between the averaged CALIPSO lidar backscatter and the first-guess model equivalent (Fig. 4.3b). As expected, the analysis provides a closer fit to the observations which is more pronounced for the analysed radar reflectivity (Fig. 4.2c). More mixed results for the cloud lidar backscatter (Fig. 4.3c) might be related to ambiguities in generating the analysis increments; increasing cloud amount at the top of the cloud to match the observations could also result in corrections of the departures at the base of the cloud due to the increased attenuation of the modelled signal leading to an excess of cloud in the model. Investigations will be done whether assimilating the whole profile rather than just when there is cloud in both model and observations might help to solve this problem.

Impact of the new observations on 4D-Var analysis when compared against own observations based on statistics for 10 days of assimilating cycling further confirmed that overall analysis is getting closer to these observations (Fig. 4.4). Note that to ensure meaningful statistics when considering variables in logarithmic space, an additional screening step is applied to the results to reject absolute departures (both AN and FG) greater than 20 dB for radar reflectivity and 10 dB for lidar backscatter. The radar reflectivity statistics clearly shows that the root mean square error (RMS) as well as bias are consistently smaller when radar and lidar observations are assimilated. Comparing to the CALIPSO data, the AN RMS is generally smaller and the magnitude of bias in AN departures is reduced in majority levels when all observations are assimilated.

Verification of the performed assimilation runs has also been carried out against other assimilated observation types in 4D-Var. The results indicated that mainly for conventional observations (such as TEMP ra-

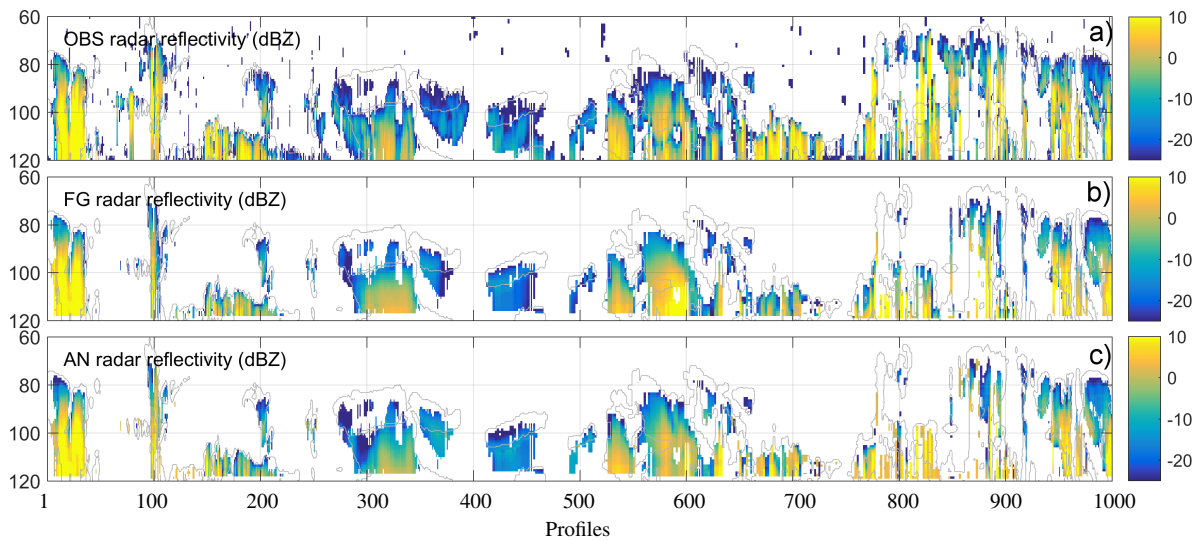


Figure 4.2: Cross-sections of radar reflectivity related variables corresponding to the portion of orbital track (21:00 UTC 31st July 2007). Panels show (a) observed CloudSat radar reflectivity (dBZ), (b) model equivalent (FG) radar reflectivity using the model background (dBZ) and (c) model equivalent (AN) radar reflectivity using the model analysis from the assimilation experiment using all observations with radar and lidar (**ALL RAD LID**). Note that the first guess radar reflectivity is only displayed where there are hydrometeors detected in both model and observations. To elucidate the position of the model clouds, the first-guess model cloud boundaries are shown in grey.

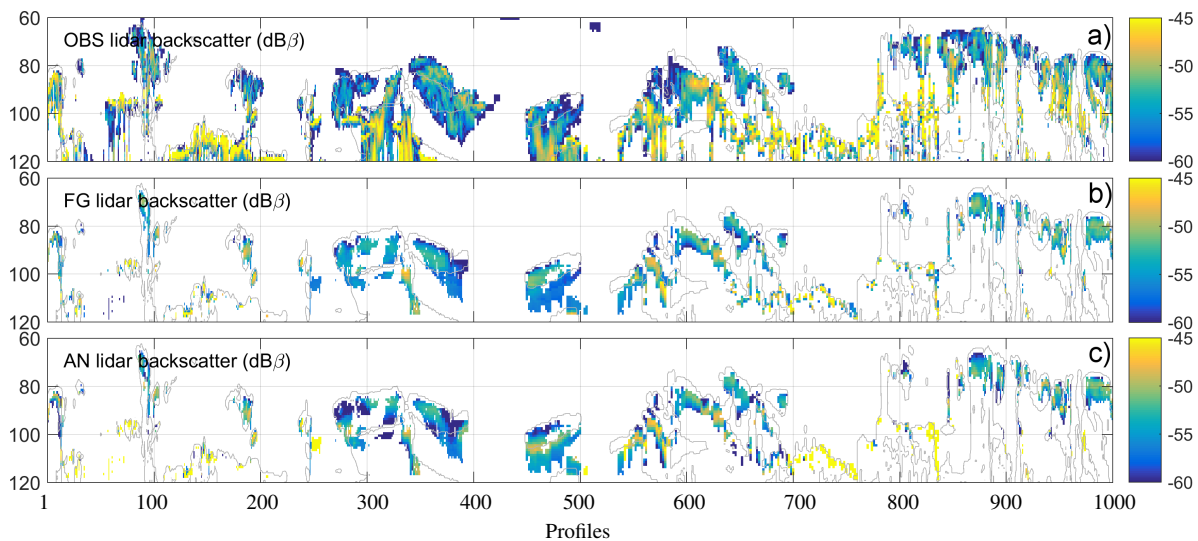
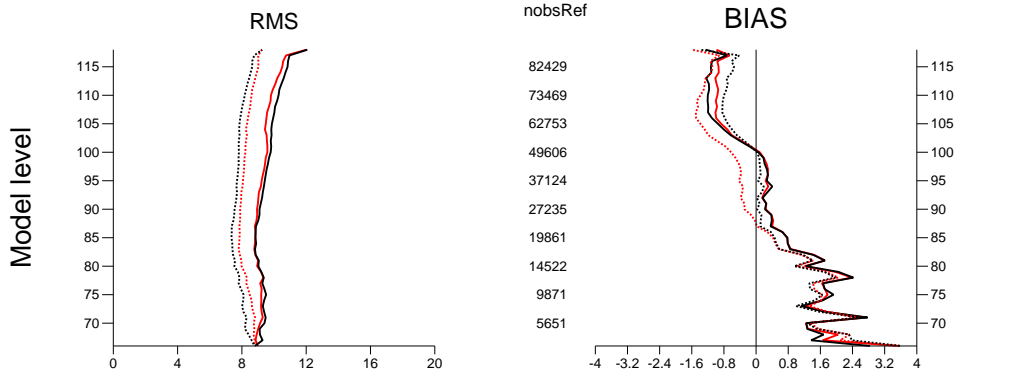


Figure 4.3: Same as Fig. 4.2, but for CALIPSO lidar backscatter.

diosonde, PILOT or AIREP observations), bias and standard deviations of the background departures are overall marginally smaller in the experimental runs compared to the reference run not using the new cloud radar and lidar observations (Fig. 4.5). The largest impact of these observations is observed for wind. For all other types of observations assimilated in 4D-Var, no significant changes have appeared when considering observations-minus-background and observations-minus-analysis departure statistics. Generally, it is not easy to achieve a significant improvement in the experimental run compared to the reference one over a domain well covered by a large amount of other measurements. Therefore any improvement is encouraging since it indicates a potential benefit from assimilating cloud information.

(a) 2007080100-2007081012(12)
 Radar reflectivity Globe
 (flag filter:230) CRADA . [gyk9(black) vs gyk8(red)]



(b) 2007080100-2007081012(12)
 Lidar Backscatter (km-1 sr-1 *10E6) Globe
 (flag filter:231) CLIDA . [gyk9(black) vs gyk8(red)]

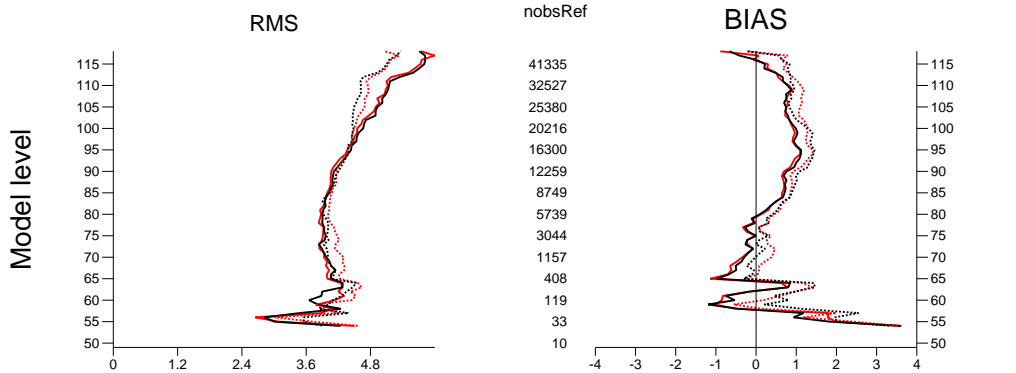


Figure 4.4: Root mean square error (left) and bias (right) of background departures (solid line) and analysis departures (dotted line) with respect to (a) cloud radar reflectivity and (b) cloud lidar backscatter observations for the reference experiment (REF, red) and experiment assimilating in addition cloud radar reflectivity and lidar backscatter observations (ALL_RAD_LID, black) using double observation errors. The number of observations for the period from 1 August 2007 00:00 UTC to 10 August 2007 12:00 UTC is displayed in the middle. Results are shown for the whole globe. The larger the model level number, the closer it is to the surface (i.e., level 117 is approximately 1km above the surface and level 70 is approximately 13 km above the surface).

4.2.2 Impact on the subsequent forecast

The evaluation of the impact of the assimilation of cloud radar and lidar observations on the skill of subsequent forecasts has been done in terms of differences in the rms forecast error between the forecasts starting from analysis assimilating these new observations and the forecast starting from the reference analysis. Both experiment's forecast errors have been computed with respect to the operational analysis. Zonal means of these rms error differences are shown for specific humidity, temperature and zonal wind in Fig. 4.6 for one assimilation cycle with the analysis time 00:00 UTC 1 August 2007. The forecast generated using the experimental analysis shows an increase in forecast skill of temperature and wind, with the greatest increases in three regions; one in the NH extra-tropics, one just north of the equator corresponding to the Inter-Tropical Convergence Zone (ITCZ), and a third in the SH extra-tropics. These three regions correspond to locations with the greatest quantity of cloud and hence radar and lidar observations.

Investigation of the forecast skill by verification of the forecast against operational analyses also indicated that while the radar provided the largest impact on forecast errors, assimilating both radar and lidar has the greatest total benefit to the forecast. In agreement with the degradation of the analysis fit to wind observations

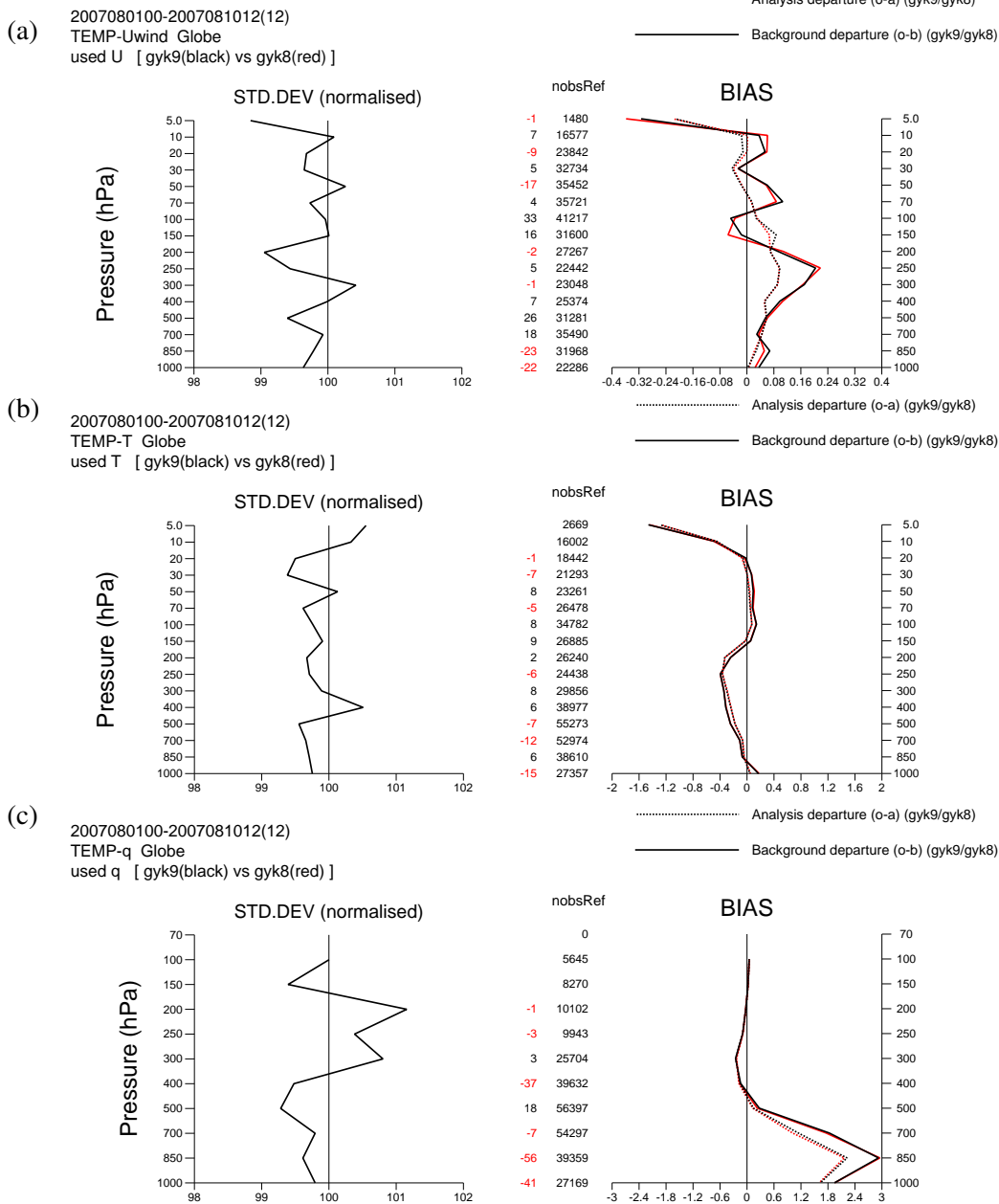


Figure 4.5: Normalised standard deviation (left) and bias (right) of background (solid line) and analysis departures (dotted line) with respect to TEMP (a) zonal wind, (b) temperature and (c) specific humidity observations for the reference run (REF, red) and experiment assimilating in addition cloud radar reflectivity and lidar backscatter observations (ALL_RAD_LID, black) using double observation errors. The number of observations for REF experiment (nobsRef) for the period from 1 August 2007 00:00 UTC to 10 August 2007 12:00 UTC is displayed in the middle together with negative red and positive black numbers indicating how many less or more, respectively, observations are used by the ALL_RAD_LID run. Results are shown for the whole globe.

when decreasing radar and lidar observation errors shown in WP-5000 (Janisková and Fielding, 2018), a clear decrease in forecast skill has been also observed. One reason for the degradation is that by decreasing the observation errors for radar and lidar, the model is forced to drawn away from other assimilated observations elsewhere in the model that contain useful information. Another reason is that fitting the model too closely to the observations can actually pull the model analysis further from the truth, particularly for profiling cloud radar and lidar observations that can have large representativity errors and uncertainties in the forward models. This highlights how much potential improvement could be gained from careful adjustments to the observation error.

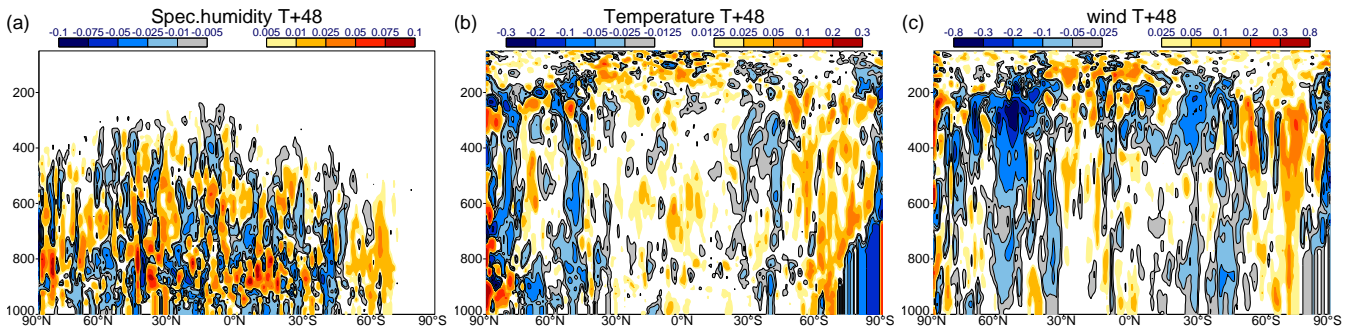


Figure 4.6: Zonal mean of differences of (a) specific humidity ($\text{g}\cdot\text{kg}^{-1}$), (b) temperature (K) and (c) wind ($\text{m}\cdot\text{s}^{-1}$) rms errors for the differences between the 48-hour forecasts starting from analysis created by 4D-Var assimilation of cloud radar reflectivity and lidar backscatter observations with doubled observation errors and the operational analysis and between the forecast starting from the reference analysis and the operational analysis. Situation **2007080100** with 12-hour assimilation period between 31 July 2007 21:00 UTC and 1 August 2007 09:00 UTC. Reduction (resp. increase) of rms errors for the experimental run is shown with blue (resp. red) shadings.

In addition to verifying forecast against model analyses, verification against observations has been also done. For longer forecast lead times the observations used in the verification are getting increasingly independent, although the observation coverage is limited compared to verifying against an analysis, so any signals are likely to require longer cycling times to remove noise. Based on 10-day assimilation cycling, forecast departures with respect to TEMP (radiosonde) observations (Fig. 4.7) indicated an increased skill in predicting tropospheric winds in the experimental run compared to the reference run for the 24 hour forecasts in the Northern hemisphere, where the observations are densest. The skill in 48 hour forecasts is reduced, but still comparable to the reference forecast. Statistics for the tropics and the Southern hemisphere are noisy, suggesting significantly more assimilation cycling is required to draw any significant conclusions. A similar pattern of increased skill in the shorter term forecasts relative to the reference has been seen in radiosonde temperature and humidity observations with the greatest improvements in the Southern hemisphere.

Assessment of rain rates in the tropics using independent observations from Tropical Measurement Mission (TRMM) has shown that the RMS in short-term surface rain rate forecasts over the tropics compared to TRMM is reduced by around 2 % when assimilating CloudSat radar reflectivity and CALIPSO lidar backscatter (Fig. 4.8). The RMS is reduced a further 1 % when using the forecasts initialised with the double error analysis, in agreement with the improved fit to other observation types (e.g., radiosonde) when using double errors.

4.3 Perspectives

The performed studies have provided indications on a potential which assimilation of cloud information from active sensors could offer. The feasibility to assimilate such observations directly into 4D-Var system in the global scale has been demonstrated for the first time. Gaining benefit on forecast skill by including new observations into a well-established observing system is extremely difficult, so the results presented here are extremely promising and warrant the opening of many avenues of further research that were not able to be explored here. The sensitivity of the results to the prescribed observation error was shown to be large and it is envisaged that relatively easy gains in forecast skill would be achievable through careful tuning. The behaviour of the assimilation system for different regimes, for example the effect of cloud radar and lidar on convective situations, requires further work and could result in improvements in the forward operator assumptions or screening criteria. No attempt was made to optimise the pre-processing of the observations, so investigations of the averaging scale and possible thinning of the observations in both the horizontal and vertical would be beneficial. Finally, investigation of the synergistic benefit of cloud radar and lidar observations to other observation types related to

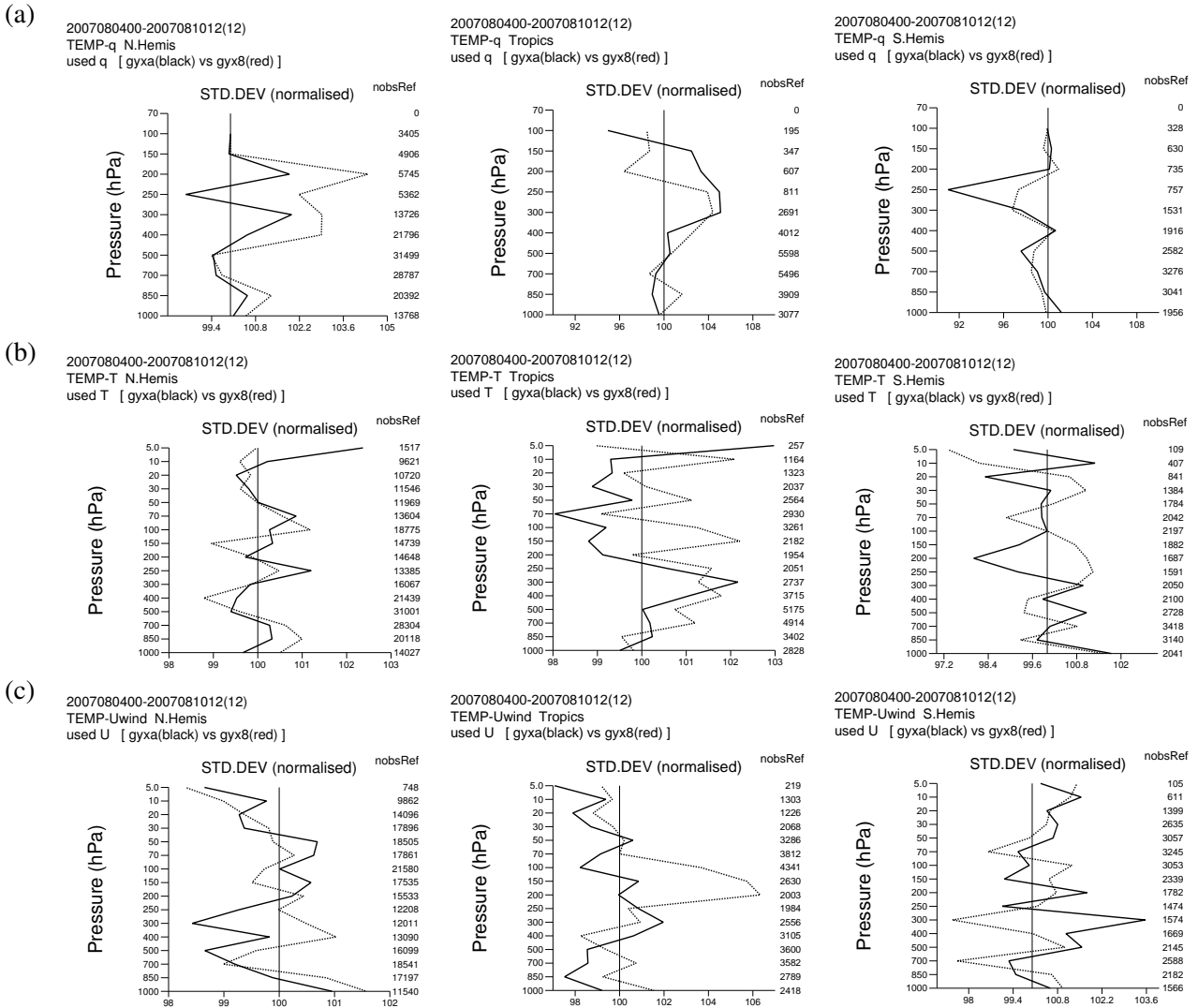


Figure 4.7: Normalised standard deviation of forecast departures with respect to TEMP (radiosonde) observations for 24h (solid line) and 48h (dotted line) forecasts shown for the experiments assimilating cloud radar reflectivity and lidar backscatter observations using double observation errors and combined with all other routinely assimilated observations. Results are shown for (left) Northern Hemisphere, (middle) Tropics and (right) Southern Hemisphere and for (a) specific humidity, (b) temperature and (c) zonal wind. The number of observations (nobsRef) for the period from 4 August 2007 00:00 UTC to 10 August 2007 12:00 UTC is displayed at the right side of each profile.

clouds, in particular the all-sky radiance assimilation framework used at ECMWF, is worthy of further research in the future.

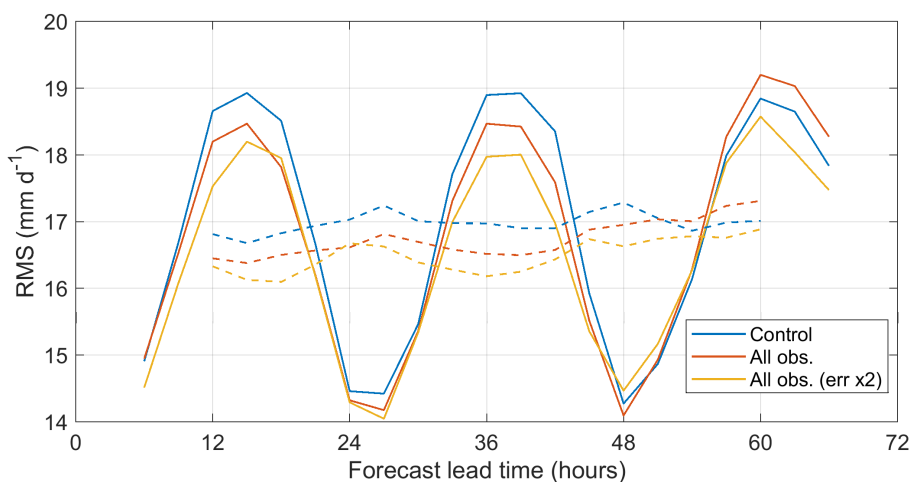


Figure 4.8: Root-mean-square error (RMS) between TRMM and forecast near-surface rain rates for varying forecast lead times of up to 3 days. Statistics are generated from forecasts initialised at 00:00 UTC and 12:00 UTC using the reference analysis (**REF**; blue) and all observations analysis (**ALL RAD LID**; red). The solid lines indicate a 12 hour averaging window, while the dashed lines indicate a 24 hour averaging window.

5 Required work towards monitoring and assimilation of EarthCARE radar and lidar observations

During the current project, whose main outcomes are summarized in Sections 2, 3 and 4, the focus was concentrated on preparing direct data assimilation and monitoring systems to exploit combined space-borne lidar and radar cloud observations for their assimilation in Numerical Weather Prediction (NWP) models. The project demonstrated the feasibility of 4D-Var assimilation of such observations using CloudSat and CALIPSO data. It thus provided necessary developments and experimentations important for further work towards preparation for the future possible operational assimilation/monitoring of the EarthCARE observations. However, the successful real-time assimilation of EarthCARE observations relies on a number of further tasks:

- For the analysis and forecast of an NWP model to gain benefit from any observations, scientific testing and tuning is necessary, particularly for new observation types.
- Additional work needs to be devoted to the optimization of the impact of space-borne cloud radar and lidar observations in an operational 4D-Var assimilation system, ensuring no degradation of the impact of other observations and forecast scores. This will involve:
 - + optimization of observation usage in data assimilation system;
 - + matching of the scale of observations and model to improve representativity of observations;
 - + tuning of observation errors and an investigation to characterise their correlation (likely to be significant in the vertical);
 - + extensions to lidar observation operator to more accurately account for multiple scattering (in ice cloud);
 - + exploration of possibility to use variational bias correction (VarBC) as a tool to treat and monitor bias;
- To expedite the tuning of the system when EarthCARE is launched, a framework for testing cloud radar and lidar observations needs to be established.

Around six months prior to launch, preparations are required to be made as details of the mission are finalised. This will include a rehearsal of the data flow where support for the communication between the operations team and the ESA ground segment will be provided. An investigation of the impact of the expected data latency in relation to cut-off times for the data assimilation needs also to be done, including the simulation of orbits. These technical preparations will allow the best possible use of the commissioning phase of the mission, where the first testing of real EarthCARE data will begin. Once the operational phase of the mission begins, on-going monitoring of measurements and their impact on the data assimilation system will need to be performed. Longer periods of the use of EarthCARE observations in the data assimilation system will allow for a comprehensive evaluation of their benefit to NWP.

Throughout the pre-launch, commissioning and operational phases an on-going effort is also required to align developments to the system related to the assimilation of cloud radar and lidar with operational model upgrades and other modifications to the data assimilation system. Without these updates, existing code can quickly become obsolete to the point that is unusable and in need of complete re-writes.

6 Brief analysis of possible benefits of using EarthCARE MSI observations for assimilation

The Multi-Spectral Imager (MSI) instrument is designed to provide a broader meteorological context to the narrow footprints of the EarthCARE radar and lidar observations. The MSI has seven spectral bands: one visible (VIS), one near-IR (NIR), two short-wave IR (SWIR) and three thermal IR (TIR). It has a swath width of 150 km with a pixel resolution of 500m, allowing it to resolve the 2D horizontal structure of clouds. Indirectly, the information could be used to provide extra information to the assimilation about the representativity of the radar and lidar observations. However, extrapolating the integrated view of the MSI to the vertically resolved profiles given by the radar and lidar is not straight-forward. Further, the observation error model currently in use based on the along-track variability is probably sufficient to determine the representativity error, so further investigations are probably not warranted. Of greater interest, therefore, is the potential for direct assimilation of the MSI radiances themselves.

Following the success of the assimilation of cloudy microwave radiances, the assimilation of TIR and SWIR channels for cloudy scenes is currently being developed and it is perceivable that, with substantial technical effort, these MSI channels could be assimilated given the availability of existing forward models such as RTTOV. Assimilating the remaining channels poses a greater challenge overall, particularly scientifically; no NWP centres currently assimilate VIS and NIR radiances. One reason for the difficulty in assimilating radiances from VIS and NIR channels historically has been the lack of suitable radiative transfer models to provide the model equivalents with sufficient speed and accuracy. However, there are fast radiative transfer models in development: the Method for Fast Satellite Image Synthesis (MFASIS; [Scheck et al., 2016](#)) based on compressed look-up tables, and the Forward-Lobe Two-Stream rAdiance Model (FLOTSAM, see [Escribano et al., in prep.](#)), which could potentially be used, although their adjoints would also need to be computed and tested.

Having stated the challenges to the direct assimilation of EarthCARE MSI observations, it is also worth mentioning the reward; the MSI radiances are expected to have a beneficial impact on synergistic retrievals of cloud and aerosol properties so should, in theory, enhance the impact of radar and lidar on the analysis and forecast. The use of instrument synergy from cloud-related observations is an emerging area of data assimilation, and is likely to grow in importance as model resolution continues to increase and clouds are better resolved in forecast models.

Acknowledgments

The authors would like to thank Robin Hogan and Stephen English for discussion on the benefits of using EarthCARE MSI observations for assimilation. The NASA CloudSat Project is kindly acknowledged for providing the CloudSat data. The authors are also grateful to the NASA Langley Research Center - Atmospheric Science Data Center for making the CALIPSO data available.

List of Acronyms

1D-Var	One-Dimensional Variational Assimilation
4D-Var	Four-Dimensional Variational Assimilation
A-NOM	ATLID Nominal data
AN	Analysis
AIREP	AIRcraft Weather REPort
ATLID	ATmospheric LIDar
BUFR	Binary Universal Form for the Representation of meteorological data
CALIOP	Cloud-Aerosol Lidar with Orthogonal Polarization
CALIPSO	Cloud-Aerosol Lidar and Infrared Pathfinder Satellite Observation
C-NOM	CPR Nominal data
CloudSat	NASA's cloud radar mission
CPR	Cloud Profiling Radar
EarthCARE	Earth, Clouds, Aerosols and Radiation Explorer
ECMWF	European Centre for Medium Range Weather Forecasts
ECSIM	EarthCARE SIMulator
ESA	European Space Agency
ESTEC	European Space Research and Technology Centre
FG	First Guess
FLOTSAM	Forward-Lobe Two-Stream rAdiance Model
IFS	Integrated Forecasting System of ECMWF
IR	Infrared
ITCZ	Inter-Tropical Convergence Zone
MFASIS	Method for Fast Satellite Image Synthesis
MSI	Multi-Spectral Imager
MODIS	Moderate Resolution Imaging Spectroradiometer
NASA	National Aeronautics and Space Administration
NH	North Hemisphere
NIR	Near Infrared
NOAA	National Oceanic and Atmospheric Administration
NWP	Numerical Weather Prediction
OBS	OBServations
PDF	Probability Distribution Function
QuARL	Quantitative Assessment of the Operational Value of Space-Borne Radar and Lidar Measurements of Cloud and Aerosol Profiles
rms/RMS	root mean square error
RTTOV	Radiative Transfer for TOVs
SH	South Hemisphere
STSE	Support-to-Science-Element
SWIR	Short-Wave Infrared
TCo639	Model cubic octahedral grid with spectral truncation T639
TIR	Thermal Infrared
TIROS	Television and Infrared Observation Satellite
TOVS	TIROS Operational Vertical Sounder
TRMM	Tropical Rainfall Measurement Mission
UTC	Universal Time Coordinated
VarBC	Variational Bias Correction
VIS	Visible (spectral band)
WP	Work Package

References

- Abel, S. J. and I. A. Boutle, 2012: An improved representation of the raindrop size distribution for single-moment microphysics schemes, *Quarterly Journal of the Royal Meteorological Society*, **138**(669), 2151–2162.
- Di Michele, S., M. Ahlgrimm, R. Forbes, M. Kulie, R. Bennartz, M. Janisková, and P. Bauer, 2012: Interpretation and evaluation of the ECMWF global model with CloudSat observations: ambiguities due to radar reflectivity forward operator uncertainties, *Q. J. R. Meteorol. Soc.*, **138**, 2047–2065, doi:10.1002/qj.1936.
- ESA, 2004: EarthCARE - Earth Clouds, Aerosol and Radiation Explorer, Reports for mission selection, the six candidate Earth explorer missions, ESA SP-1279, ESA Publications Division c/o ESTEC, Noordwijk, The Netherlands.
- Escribano, J., A. Bozzo, P. Dubuisson, J. Flemming, R. J. Hogan, L. Labonnote, and O. Boucher, in prep.: A benchmark for testing the accuracy and computational cost of shortwave top-of-atmosphere reflectance calculations in clear-sky aerosol-laden atmospheres, *GMD*.
- Fielding, M. and M. Janisková, 2017a: Observation quality monitoring and pre-processing, WP-2000 report for the project Operational Assimilation of Space-borne Radar and Lidar Cloud Profile Observations for Numerical Weather Prediction, ESA ESTEC contract 4000116891/16/NL/LvH, 61 pp.
- Fielding, M., M. Janisková, and R. Hogan, 2017: EarthCARE data handling and testing, WP-4000 report for the project Operational Assimilation of Space-borne Radar and Lidar Cloud Profile Observations for Numerical Weather Prediction, ESA ESTEC contract 4000116891/16/NL/LvH, 29 pp.
- Fielding, M. D. and M. Janisková, 2017b: Observation quality monitoring and pre-processing, WP-2000 report for the project Operational Assimilation of Space-borne Radar and Lidar Cloud Profile Observations for Numerical Weather Prediction, 4000116891/16/NL/LvH, pp.
- Illingworth, A. et al., 2015: The earthcare satellite: The next step forward in global measurements of clouds, aerosols, precipitation, and radiation, *Bulletin of the American Meteorological Society*, **96**(8), 1311–1332.
- Janisková, M., S. Di Michele, and E. Martins, 2014: Support-to-Science-Elements (STSE) Study - EarthCARE Assimilation, ESA Contract Report on Project 4000102816/11/NL/CT, 225 pp.
- Janisková, M. and M. Fielding, 2018: Feasibility demonstration of 4D-Var assimilation system using CloudSat and CALIPSO observations, WP-5000 report for the project Operational Assimilation of Space-borne Radar and Lidar Cloud Profile Observations for Numerical Weather Prediction, ESA ESTEC contract 4000116891/16/NL/LvH, 35 pp.
- Janisková, M., M. Fielding, M. Crepulja, D. Vasiljević, T. Král, and P. Lean, 2017: Assimilation system development for cloud radar and lidar observations, WP-3000 report for the project Operational Assimilation of Space-borne Radar and Lidar Cloud Profile Observations for Numerical Weather Prediction, ESA ESTEC contract 4000116891/16/NL/LvH, 26 pp.
- Janisková, M., O. Stiller, S. Di Michele, R. Forbes, J.-J. Morcrette, M. Ahlgrimm, P. Bauer, and L. Jones, 2010: QuARL - Quantitative Assessment of the Operational Value of Space-Borne Radar and Lidar Measurements of Cloud and Aerosol Profiles, ESA Contract Report on Project 21613/08/NL/CB, 329 pp.
- Kulie, M. S., R. Bennartz, T. J. Greenwald, Y. Chen, and F. Weng, 2010: Uncertainties in microwave properties of frozen precipitation: implications for remote sensing and data assimilation, *J. Atmos. Sci.*, **67**, 3471–3487.

- Scheck, L., P. Frèrebeau, R. Buras-Schnell, and B. Mayer, 2016: A fast radiative transfer method for the simulation of visible satellite imagery, *Journal of Quantitative Spectroscopy and Radiative Transfer*, **175**, 54–67.
- Stephens, G., D. Vane, R. Boain, G. Mace, K. Sassen, Z. Wang, A. Illingworth, E. O’Connor, W. Rossow, and S. Durden, 2002: The CloudSat mission and the A-train, *Bull. Am. Meteorol. Soc.*, **83(12)**, 1771–1790.
- Stiller, O., 2010: A flow-dependent estimate for the sampling error, *J. Geophys. Res.*, **115 (D22)**, doi: 10.1029/2010JD013934.
- Winker, D., M. Vaughan, A. Omar, Y. Hu, K. Powell, Z. Liu, W. Hunt, and S. Young, 2009: Overview of the CALIPSO mission and CALIOP data processing algorithms, *J. Atmos. and Ocean. Tech.*, **26(7)**, 2310–2323.